IMPLEMENTATION AND EVALUATION OF A FREQUENCY-BASED CURRENT-SHARING TECHNIQUE FOR CELLULAR CONVERTER SYSTEMS

David J. Perreault Robert L. Selders, Jr John G. Kassakian

Massachusetts Institute of Technology
Laboratory for Electromagnetic and Electronic Systems
Cambridge, MA 02139 USA

ABSTRACT

The paper presents the implementation and experimental evaluation of a new current-sharing technique for paralleled power converters. This technique is based on frequency encoding of the current-sharing information, and requires no inter-cell connections for communicating this information. Practical implementation of the approach is addressed, and an experimental evaluation of the approach based on a three-cell prototype system is also presented. It is shown that accurate and stable load sharing is obtainable over a wide load range with this approach.

INTRODUCTION

Large power converter systems are sometimes constructed using a *cellular* architecture, in which many quasi-autonomous converter cells are paralleled to form a single large converter (Fig. 1). Advantages of the cellular architecture include modularity, improved reliability and performance, and the ability to achieve high power levels [1,2].

One challenge in realizing a paralleled converter architecture is the implementation of a current-sharing mechanism which causes all of the converter cells to share the load current equally and stably. This is commonly done by interconnecting the cells through a communications bus [3-10]. However, the use of such additional interconnections among cells is undesirable in many applications for reliability reasons, especially when the system is comprised of a large number of cells.

The paper presents the implementation and experimental evaluation of a recently proposed current-sharing approach which requires no additional interconnections among cells [11]. In this approach, each cell encodes load-sharing information onto the output bus at frequencies much higher than the fundamental output frequency of the converter system and much lower than the system switching frequency. The aggregated information is then used by the individual cells for distributed load-sharing control. Section 2 of the paper describes the operation of the current-sharing approach. One possible implementation of the approach is detailed in section 3, including methods for encoding and decoding current-sharing information. The design of a low-power prototype system employing this approach is also described. Section 4 presents an experimental evaluation of the current-sharing approach using this prototype cellular converter, and the final section concludes the paper.

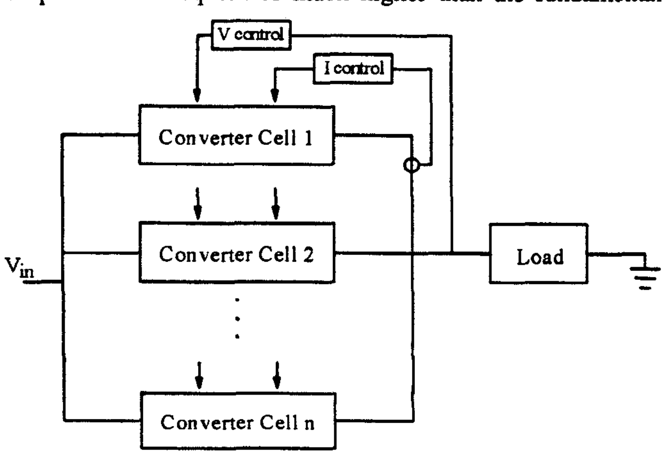

Figure 1 A cellular converter architecture supplying a single load.

CURRENT-SHARING CONTROL

We consider the output-perturbation method of current-sharing control proposed in [11]. In this method, each cell superimposes a small, high-frequency perturbation onto its output current. The magnitude and frequency of the perturbation is controlled as a function of the cell reference current (or some other variable to be regulated). The frequency content of the output voltage perturbation resulting from the aggregated current perturbations contains information about the cell output currents, and is measurable by each cell.

To effect current sharing, each cell employs a frequency estimator to calculate a weighted rms average, ω_{est}, of the output perturbation frequency content. This estimate has the form

$$\omega_{est} = \frac{\sqrt{\sum_{k=1}^{N} m_k^2 \omega_k^2}}{\sqrt{\sum_{k=1}^{N} m_k^2}} \qquad (1)$$

where m_k and ω_k are the magnitude and frequency of the output perturbation due to the k^{th} cell. Each cell compares its own perturbation frequency to the estimated average and adjusts its output such that its own perturbation frequency approaches the average. As the individual perturbation frequencies approach a single average value, the individual output currents will also approach a single value, achieving the desired load balance. For example, in a dc output supply, load balance can be achieved if each cell adjusts its local reference voltage according to the difference between the local perturbation frequency and the estimated rms frequency.

PROTOTYPE SYSTEM IMPLEMENTATION

Here we describe a full implementation of this current-sharing

0-7803-3019-6/96/$3.00 © 1996 IEEE.

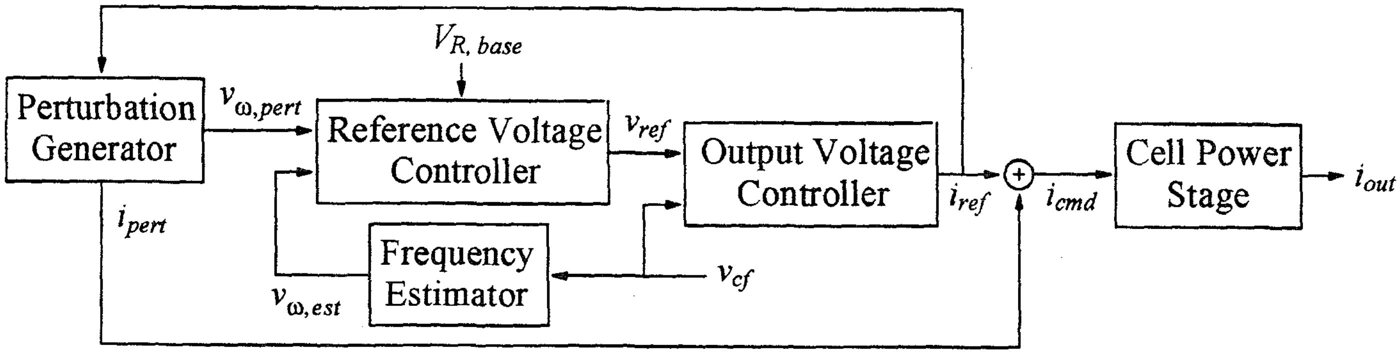

Figure 2 Block diagram of the cell control structure.

scheme using low-power buck converter cells operating under current-mode control. In simplest terms, each cell can be viewed as having an inner current control loop, a middle voltage control loop, and an outer load-sharing control loop. Implementation of the outermost loop with the perturbation method requires that each cell encode information about its current onto the output (via a perturbation generator) and decode the aggregated information from the output (via a frequency estimator). We will describe methods and circuits for generating the proper perturbation signals, estimating the rms perturbation frequency from output voltage measurements, and controlling the load balance among cells.

The structure of an individual cell implementing the perturbation method is illustrated in Fig. 2. The converter cell power stage generates an output current whose peak value is equal to the peak commanded current i_{cmd}. The commanded current is the sum of a reference current i_{ref}, generated by the output voltage controller, and a perturbation signal i_{pert}, generated by the perturbation generator circuit. The output voltage controller generates i_{ref} based on the difference between the output voltage v_{cf} and the reference voltage v_{ref}. The load-sharing controller adjusts v_{ref} based on the difference between the local perturbation frequency and the rms perturbation frequency calculated by the frequency estimator circuit. These subsystems operate together to regulate the output voltage while maintaining the desired load balance among cells.

Prototype System Power Stage

A three-cell low-power buck converter system was constructed as a test bed. The buck converter cells ($f_{sw} \approx 200$ kHz, $L \approx 125$ mH) are designed to regulate the output to an adjustable reference of approximately 5.1 V from an input voltage of approximately 15 V. The individual cells are designed to supply a full load output current of 25 mA, yielding a total load range of 5 to 75 mA. The system has an output filter capacitance of 0.33 μF, and is resistively loaded.

The individual cells are operated under current-mode control using the UC3843 current-mode control chip. The internal current-sense comparator and error amplifier are overridden and replaced with external circuitry to allow direct control of the commanded peak turn-off current, i_{cmd}.

Perturbation Generation

The prototype perturbation generator circuit implements an incrementally linear relationship between cell reference current and perturbation frequency, with cell currents from no load to full load yielding perturbation frequencies from 5 to 10 kHz. The perturbation frequency range is selected to be well below the 200 kHz cell switching frequency, but well above the output voltage control bandwidth of the system (~100 Hz). The perturbation magnitude is selected to be proportional to the perturbation frequency, with a maximum magnitude of approximately 0.25 mA at 10 kHz. This is done to yield output voltage perturbations (across the capacitive output filter) which are approximately constant in magnitude across frequency. The selected magnitude range yields very small (<1%) output voltage ripple for the three-cell system.

The perturbation generator is implemented using an XR2206 monolithic function generator, which contains a voltage-controlled oscillator (VCO) and sine-wave shaping circuitry. The VCO input allows control of the perturbation frequency, and an amplitude modulation input allows easy control of the perturbation magnitude. The generated perturbation signal is superimposed on the reference current, and the result is supplied to the current-mode PWM controller.

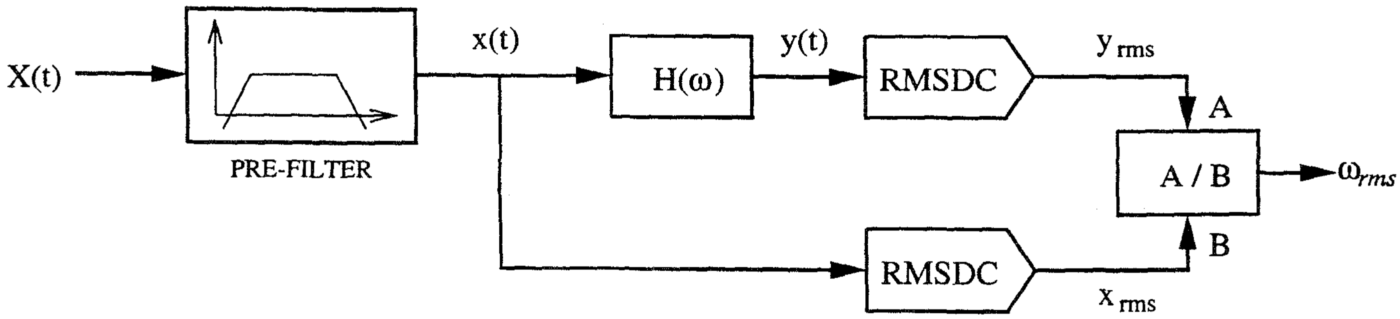

Figure 3 A circuit structure for computing the rms frequency estimate of the aggregate signal.

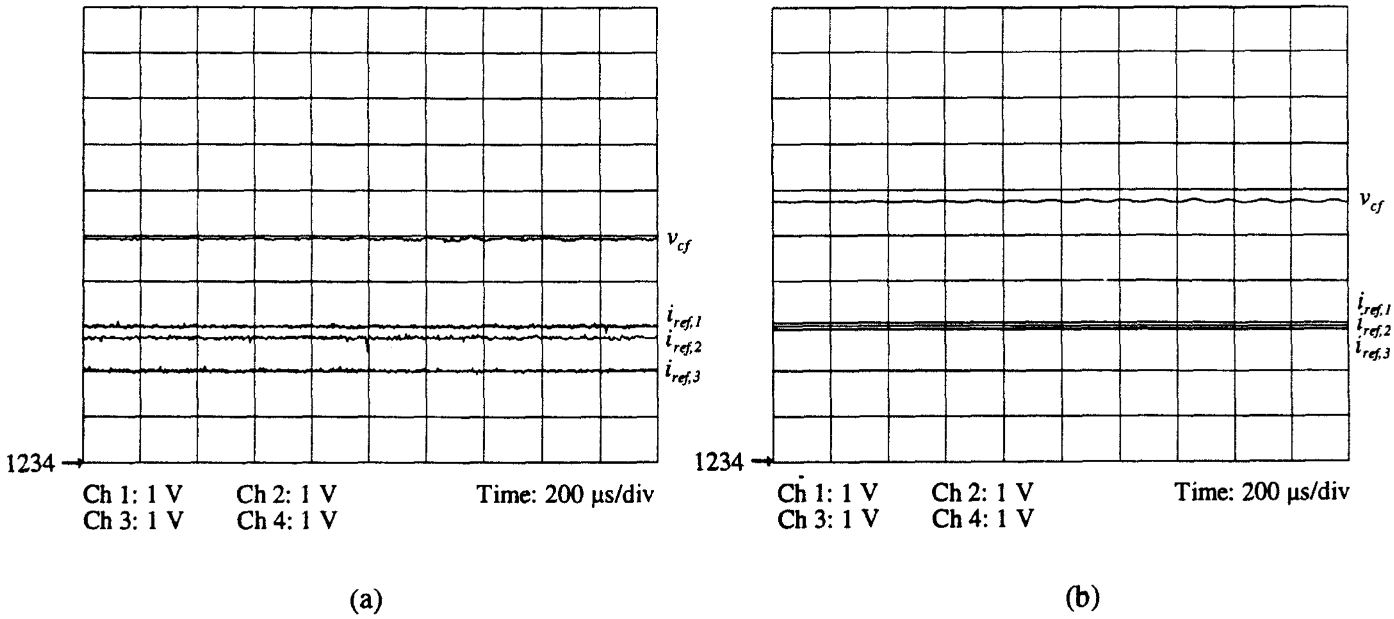

Figure 4 Load-sharing characteristics of the prototype system at approximately 60% of full load ($R_{load} \approx 133\ \Omega$). (a) Without load-sharing control. (b) With load-sharing control.

Frequency Estimation

To achieve load balance, each cell compares its own perturbation frequency to the rms of all the perturbation frequencies. It is shown in [11] that the rms perturbation frequency can be estimated from the output voltage using the structure of Fig. 3, with $H(\omega) = j\omega$. The estimator is composed of four sections: (1) a bandpass filtering stage, (2) a gain and band-limited differentiation stage, (3) an integrated circuit rms-to-dc conversion stage, and (4) a division stage. The bandpass filtering stage is implemented as a cascade of a second-order high-pass Butterworth filter, a fixed gain, and a second order low-pass Butterworth filter. The corner frequencies are set to 500 Hz and 20 kHz, in order to block out both the low-frequency and switching-frequency components of the output voltage. The differentiation stage consists of a band-limited differentiator circuit which generates the derivative for frequency components in the range of interest, but is gain limited above approximately 50 kHz to limit the amplification of high frequency noise. The rms-to-dc conversion stage is implemented using AD637 integrated circuit rms-to-dc converters connected in the two-pole Sallen-Key filter arrangement. The averaging and filter capacitor values ($C_{AV} = 0.022\ \mu F$, $C_2 = C_3 = 0.047 \mu F$) are selected to yield a 1% settling time of 8 msec, which represents a good tradeoff between frequency resolution and response speed (see [11] for an analysis of this tradeoff). The division stage is composed of a four quadrant multiplier placed in the feedback path of an operational amplifier. This approach is typically less expensive than the use of a logarithm-based division circuit, but requires careful attention to the compensation of the nonlinear feedback loop. The division stage also incorporates an output scale and offset compensation circuit for improved accuracy. The prototype estimator employs only simple, low-cost circuitry, and has sufficient accuracy to achieve a high degree of current sharing.

Control Design

For the parameters of the prototype system, a cell under peak current-mode control can be modeled as a controlled current source of the value of the peak commanded current. To achieve output voltage control, a high-gain, single-pole compensator (Gain = 125 mA/V, $\tau = 0.18$ sec) is used to generate the peak control current from the error between the reference voltage and the output voltage. This yields an output voltage control bandwidth on the order of tens of Hertz and a small but nonzero cell output impedance.

Load balance among cells is controlled by adjusting the local cell reference voltages within limits about a base value. Each cell has a high gain, single-pole compensator (Gain = 10 V/kHz, $\tau = 33.6$ sec) which generates a reference voltage adjustment based on the difference between the estimated rms perturbation frequency and the cell perturbation frequency (Fig. 2). This yields a load-sharing bandwidth of on the order of Hertz (much slower than the voltage control loop) and a small but nonzero steady-state load-sharing error.

EXPERIMENTAL EVALUATION

Here we evaluate the new load-sharing control approach using a 3-cell prototype system of the presented design. Figure 4 shows the load-sharing behavior at approximately 60% load both with and without the load-sharing control. Without load-sharing control, a 3:2 imbalance between the highest and lowest cell currents is observed, with much worse imbalances sometimes occurring depending on the individual cell reference voltages and output impedances. With load-sharing control, the cell currents are all balanced within 3% of their average. (We point out that the perturbation method yields accurate load-sharing *regardless* of how the cells share current without active control.) This high degree of load sharing is achieved using only very small (<1%) perturbations in output voltage to encode current-sharing information (Fig. 5).

Figure 6 shows the static load-sharing behavior of the system over the whole load range, while Fig. 7 shows the load regulation characteristic of the converter system over the load range. The load sharing is quite good over the entire range, but is better at

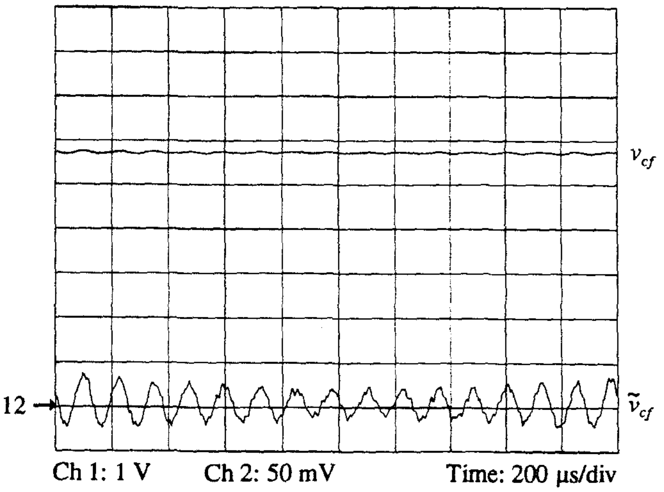

Figure 5 The output voltage and its ac perturbation component at approximately 60% of full load.

heavier loads both in absolute terms and as a percent of total current. (We point out that while good current sharing is desirable over the whole load range, it is much more important at heavier loads, where the cells are under higher stress.) Current sharing limitations are primarily due to the accuracy of the frequency estimators and the perturbation generators. The frequency estimator circuits have an absolute accuracy of about ±250 Hz over the 5 - 10 kHz range, which corresponds to an absolute current error of about ±1.25 mA. This maximum absolute error becomes more significant as a percentage at lighter loads. Furthermore, the estimators tended to be more accurate at frequencies above 8 kHz, leading to smaller absolute errors at heavier loads. Nevertheless, these results demonstrate that accurate static current sharing can be obtained over a wide load range with this approach.

Load-sharing behavior was also investigated under transient conditions. Figure 8 shows the current-sharing behavior for load steps between 681 Ω and 74 Ω, corresponding to approximately 10% and 100% of full load . (Figure 9 shows the frequency spectrum of the output voltage perturbations used to achieve current sharing at these load values.) The current-sharing behavior is seen to be very stable for even large load steps.

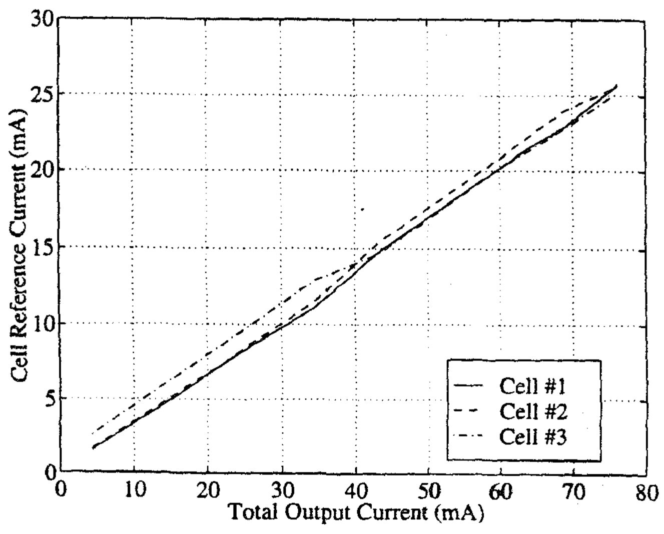

Figure 6 Static load-sharing characteristic of the prototype system.

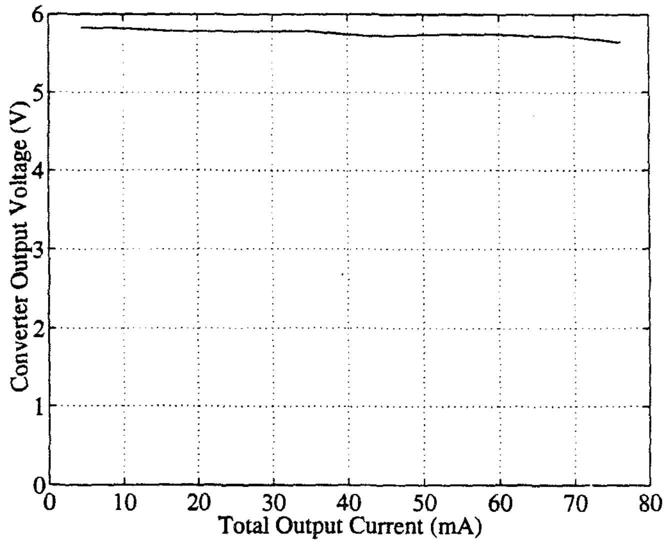

Figure 7 Load-regulation characteristic of the prototype system.

Figure 10 shows the response to a current-sharing disturbance for two cells operating at approximately 30% of full load. The dynamic response to current-sharing errors is also seen to be well behaved. What may be concluded from these results is that the presented output perturbation method can be used to achieve accurate static and dynamic load sharing without the need for additional interconnections among cells.

CONCLUSION

This paper presents the implementation and experimental evaluation of a new current-sharing approach for paralleled power converters. This approach, which is based on frequency encoding of current-sharing information, eliminates the need for additional current-sharing interconnections among converters. Practical implementation of the approach is addressed, including methods and circuits for perturbation generation, rms frequency estimation, and distributed load-sharing control. An experimental evaluation of the new current-sharing approach based on a 3-cell prototype system is also presented. It is shown that accurate load-

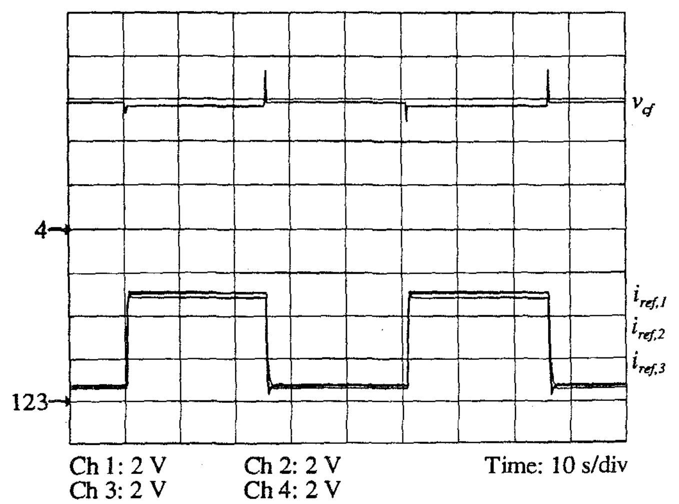

Figure 8 Current-sharing behavior for load steps between 681 Ω and 74 Ω (approximately 10% and 100% of full load).

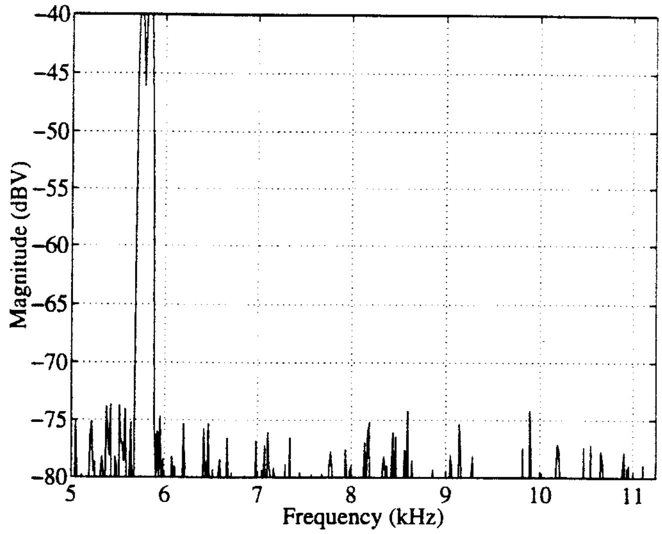

(a)

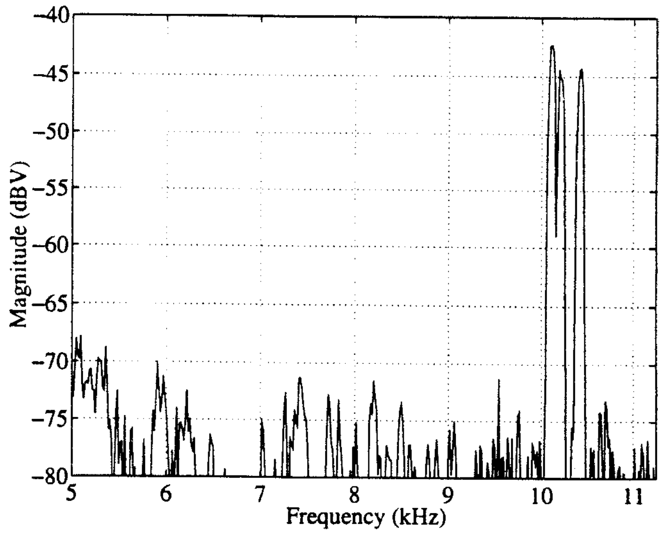

(b)

Figure 9 Frequency spectra of the output voltage perturbations used to achieve load sharing. (a) R_{load} = 681 Ω (approximately 10% of full load). (b) R_{load} = 74 Ω (approximately 100% of full load).

sharing is obtainable over a wide load range using this approach.

ACKNOWLEDGMENTS

The authors would like to gratefully acknowledge support for this research from the Bose Foundation. Generous equipment grants from the Intel and Tektronix Corporations facilitated this research. David Perreault gratefully acknowledges support from an IEEE Convergence Fellowship in Transportation Electronics, and Robert Selders thanks Delco Electronics for support through the Delco Electronics scholarship program.

REFERENCES

[1] J.G. Kassakian, "High Frequency Switching and Distributed Conversion in Power Electronic Systems," *Sixth Conference on Power Electronics and Motion Control (PEMC 90)*, Budapest, 1990.

[2] J.G. Kassakian and D.J. Perreault, "An Assessment of Cellular Architectures for Large Converter Systems," *First International Conference on Power Electronics and Motion Control*, Beijing, 1994, pp. 70-79.

[3] K.T. Small, "Single Wire Current Share Paralleling of Power Supplies," *U.S. Patent 4,717,833*, 1988.

[4] R. Wu, T. Kohama, Y. Kodera, T. Ninomiya, and F. Ihara, "Load-Current-Sharing Control for Parallel Operation of DC-to-DC Converters," *IEEE Power Electronics Specialists Conference*, 1993, pp. 101-107.

[5] T. Kohama, T. Ninomiya, M. Shoyama, and F. Ihara, "Dynamic Analysis of Parallel-Module Converter System with Current Balance Controllers," *IEEE International Telecommunications Energy Conference*, 1994, pp. 190-195.

[6] T. Kohama, T. Ninomiya, M. Wakamatsu, and M. Shoyama, "Static and Dynamic Response of a Parallel-Module High Power-Factor Converter System with Current-Balancing Controllers," *IEEE Power Electronics Specialists Conference*, 1996, pp. 1198-1203.

[7] M. Jovanovic, D. Crow, and L. Fang-Yi, "A Novel, Low-Cost Implementation of 'Democratic' Load-Current Sharing of Paralleled Converter Modules," *IEEE Trans. Power Electron.*, Vol. 11, No. 4, July 1996, pp. 604-611.

[8] V.J. Thottuvelil and G.C. Verghese, "Stability Analysis of Paralleled DC/DC Converters with Active Current Sharing," *IEEE Power Electronics Specialists Conference*, 1996.

[9] D. Maliniak, "Dense DC-DC Converters Actively Share Stress," *Electronic Design*, Jan. 21, 1993, pp. 39-44.

[10] M. Jordan, "UC3907 Load Share IC Simplifies Parallel Power Supply Design," *Unitrode Application Note U-129*, Unitrode Corp., Merrimack, NH.

[11] D.J. Perreault, R.L. Selders, Jr., and J.G. Kassakian, "Frequency-Based Current-Sharing Techniques for Paralleled Power Converters," *IEEE Power Electronics Specialists Conference*, 1996.

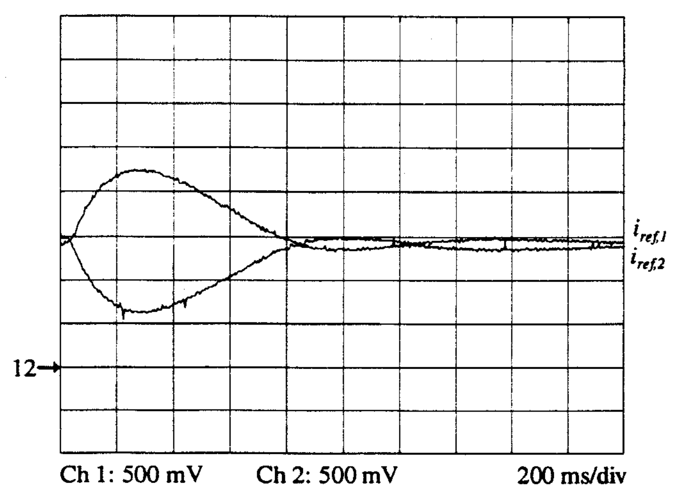

Figure 10 Dynamic response to a current-sharing perturbation for two cells operating at approximately 30% of full load.